Comparative Analysis of Single and Three-phase Dual Active Bridge Bidirectional DC-DC Converter Based on the Phase-Shifting Control

Gangui Yan, Yonglin Li* and Qi Jia
Department of Electrical Engineering, Northeast Dianli University, Chuanying District, Jilin 132012, China
*Corresponding author

***Abstract*—In order to analyze and compare the operating characteristics of high frequency isolated single and three-phase DC-DC converters under the same traditional control method. Firstly, comparisons on single-phase dual active bridge bidirectional DC-DC converter (DAB) and three-phase DAB based on the traditional phase-shifting control were carried out, operating principles of single and three-phase DAB under the traditional phase-shifting control were introduced in detail and analysis on operation modes was provided. Secondly, mathematical models of the transmitted power and backflow power of single and three-phase DAB were built. Through analysis, it is showed that, under same transmitted power, the three-phase DAB has lower backflow power and higher power transmission efficiency. Lastly, simulation models of single and three-phase DAB were built in EMTDC/PSCAD to verify the operating principles and transmitted power of single and three-phase DAB and the relative sizes of their backflow power.**

Keywords-phase-shifting control; single-phase DAB; three-phase DAB; transmission power; backflow power

I. INTRODUCTION

With the development of smart power grid, power conversion system (PCS) has played an increasingly important role in power conversion of power grid access like distributed power supply and energy storage as well as flexible transmission [1]. Voltage matching and electrical blocking among all kinds of systems are realized through power frequency isolating transformer in various existing PCS solutions [2-3]. However, defects like large volume and big noise, et al. has restricted development of PCS in smart power grid, while the high-frequency isolated bidirectional DC-DC converter (IBDC) featuring strengths in small volume, light weight and low cost has been paid more and more attentions [1]. In addition to the above strengths, it also has easy-to-realize soft switch, bidirectional energy flow, small voltage and current stress of components, large power density, and high efficiency, et al. The converter has been widely applied in occasions like power electronic transformer [4], new energy power generation [5-7] and super-capacitor energy storage, et al.

IBDC was put forward in 1991, but limited by power components and magnetic materials at that time, it failed to develop. What's worse, its efficiency was far from reaching actually-applied level due to large circuit loss caused by high-frequency characteristic of IBDC. IBDC has again raised scholars' attentions in recent years with advancements in emerging power components and nanometer porcelain materials.

There are many IBDC topological structures. According to the amount of transistors, it can be divided into dual-transistor structure like two-transistor fly-back IBDC; three-transistor structure like direct-reverse fly-back IBDC; four-transistor structure like dual push-pull IBDC; five-transistor structure like full-bridge fly-back IBDC; six-transistor structure like half-bridge/ full-bridge IBDC and eight-transistor structure like dual active-active full-bridge IBDC (DAB-IBDC). When voltage and current grade of a switching tube remain constant, power transmitted capability of IBDC is proportional to the amount of switch transistors. Therefore, DAB-IBDC possesses the largest power transmitted capability.

At present, researches on IBDC both at home and abroad are mainly concentrated in topological structure, control method and basic operation characteristics, et al. of single-phase DAB. Operation modes analysis and working efficiency of single-phase DAB have been compared in [8] under traditional control and dual-shift phase control method of modal analysis and working efficiency, which concluded that the dual-shift phase control could better solve the problem of single-phase DAB backflow power, improving efficiency of single-phase DAB. Selection method of dual-shift phase angle in the minimum backflow power under dual-phase shift control has been analyzed on the basis of [8] and an optimal strategy of backflow power has been also put forward in [9]. Turn-off loss of power components can be reduced based on resonance and different optimal methods can be used for optimizing resonance network parameters of single-phase DAB in [10-11]. A kind of high-voltage gain bidirectional DC-DC converter applied to DC micro grid has been proposed in [12]. A star-triangle three-phase high-frequency DC transformer structure has been adopted in the converter. The influence of different wiring methods for high-frequency transformers in three-phase DAB on operational characteristics of three-phase DAB has been considered in [13]. A voltage source type of push-pull three-phase DC-DC converter has been proposed in [14, 15]. There are total 6 power components in primary and secondary sides of the converter. A magnetic core has been shared by three-phase transformer, which has effectively improved the utilization rate of the magnetic core and largely downsized the

transformer. But there is no comparison between single-phase DAB and three-phase DAB conducted and imperfect research has been performed in [12-15].

In summary, the paper with dual active full-bridge IBDC as the research object has a comparative analysis on operating principles of single and three-phase DAB under the traditional phase-shifting control, which has also established mathematical models of transmitted power and backflow power for single and three-phase DAB, respectively. Simulation models of single and three-phase DAB are finally built in EMTDC/PSCAD to verify the operating principles, transmitted power and the relative size of their backflow power ratio.

II. OPERATING PRINCIPLES OF CONVERTERS

A. Principles of the Traditional Phase-Shifting Control

Figure I is a circuit topological structure for single and three-phase DAB. Single-phase DAB is mainly composed of two full-bridge converters, two DC capacitors, an auxiliary induction and a high-frequency transformer, as shown in Figure I(a). Structure of three-phase DAB is similar to that of single-phase DAB as shown in Figure I(b). And Y-Y wiring form is adopted in three-phase high-frequency transformer.

In Figure I(a), U_1 and U_2 are DC voltage of both sides of H_1 and H_2 bridges, respectively. L_1 is the sum for series connection between leakage inductance and auxiliary induction of the high-frequency transformer. Switching frequencies on both sides of H_1 and H_2 are the same during working process of single-phase DAB. Full-bridge diagonal switches of both sides are conducted in turns at the angle of 180 degrees. Full-bridge invert output voltage u_{h1} and u_{h2} of both sides are the square wave voltage with duty ratio of 50%. Voltage sizes and flow directions of both sides of inductance L_1 can be controlled via controlling phase angle among square waves. Thus, sizes and flow directions of power can also be controlled. Power transmitting from U_1 side to U_2 side is taken as an example to carry out analysis in the paper, that is, phase position of u_{h1} exceeding u_{h2}, operating waveforms of single-phase DAB can be obtained under traditional shift phase, as shown in Figure II(a).

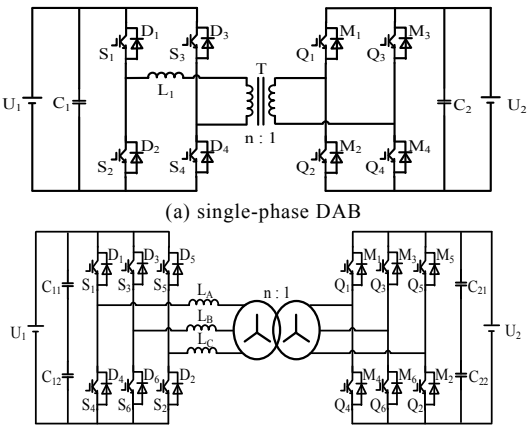

(a) single-phase DAB

(b) three-phase DAB

FIGURE I. CIRCUIT TOPOLOGIES OF CONVERTERS

In Figure II(a), U_1 and U_2 are DC voltages of both sides of H_1 and H_2 bridge, respectively; u_{h1} is full-bridge invert output voltage of U_1 side; u_{h2} is the voltage obtained upon full-bridge invert output voltage of U_2 side converted into U_1 side; n is transformation ratio of the transformer; T_{hs} is half of a switching period; D is the shift phase ratio within half of the switching period, $0 \le D \le 1$; Driving signals of switching transistor S_1 is represented by its name S_1 for convenience; Likewise, other switching transistors are represented in the same way.

The stage that inductive current is in the opposite phase position of the voltage of original side, that is, t_0—t_0' stage shown in Figure II(a). During this period, the transmitted power being negative flows back to the power source which is defined as backflow power in [9]. From the Figure II(a), when the transmitted power is constant, backflow power increases to compensate for the period of power; amount of positive transmitted power also increases, leading to increase in converter power circulation and current stress. It also increases the loss of power components and magnetic elements, reducing efficiency of the converter.

Similar to single-phase DAB operation modes, three-phase DAB also adopts the traditional phase-shifting control method. Conductive angle of each bridge arm is 180 degrees; Up and down arms of the same half bridge. Successive angles of conduction for each phase has a 120-degree difference. Size and flow direction imposed on both ends of series inductance can be controlled through controlling phase angles among square waves. Unlike single-phase DAB, three-phase DAB is divided into two different situations, that is, $0<\varphi<\pi/3$, $0<D<1/3$ and $\pi/3<\varphi<2\pi/3$, $1/3<D<2/3$. Thus, analysis is conducted by taking A-phase power transmitted from U_1 side to U_2 side as an example, that is, phase position of u_{h1A} exceeding u_{h2A}, operating waveforms of three-phase DAB under traditional shift phase control method can be obtained during two different situations as shown in Figure II(b) and (c).

Differing from Figure II(a), u_{h1A} is the A-phase invert output voltage of U_1 side; u_{h2A} is the voltage obtained upon full-bridge invert output voltage of U_2 side converted into U_1 side. It can be seen from the waveforms that backflow power is also existed in the power transmission process due to existence of displacement between u_{h1A} and u_{h2A}, as shown t_0—t_0' in Figure II(b) and t_0—t_0' in Figure II(c).

B. Operation Modes Analysis of Three-Phase Dual Active Bridge Bi-Directional DC-DC Converter

Detailed analysis is conducted on working characteristics of single-phase DAB in [9]. So, three-phase DAB will be studied in this chapter. Assuming that the converter has been working in a sTable state, working modes of the converter can be separated into six states in an half period under the first situation of $0<\varphi<\pi/3$, $0<D<1/3$ and the second situation of $\pi/3<\varphi<2\pi/3$, $1/3<D<2/3$, according to the waveforms of operating principles of three-phase DAB under the phase-shifting control which is shown in Figure II. A phase is taken as an example to analyze each working state. Specific analysis results are presented in Table I and Table II:

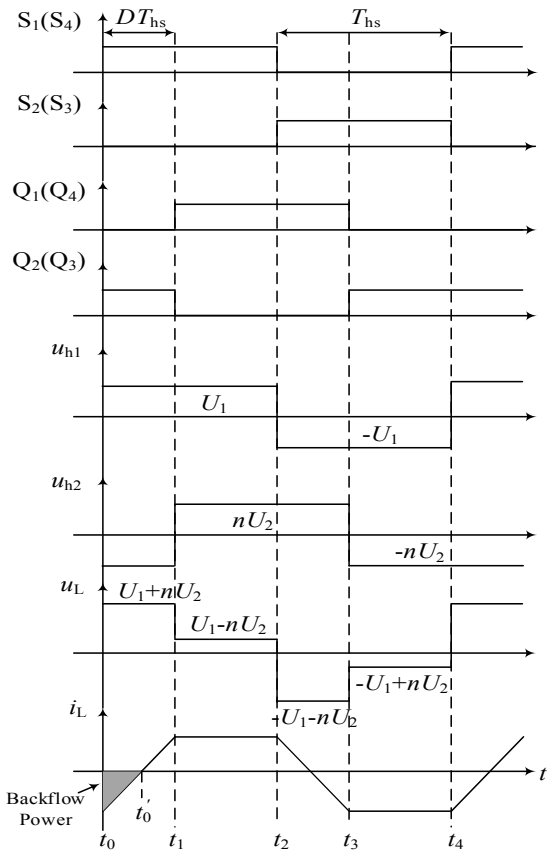

(a) single-phase DAB

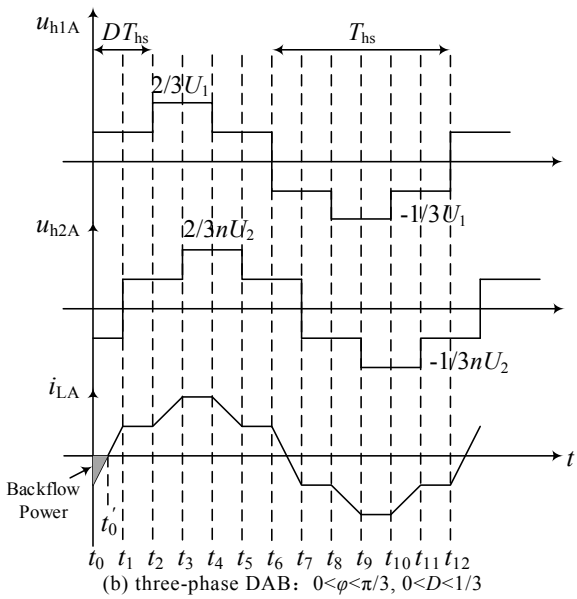

(b) three-phase DAB：0<φ<π/3, 0<D<1/3

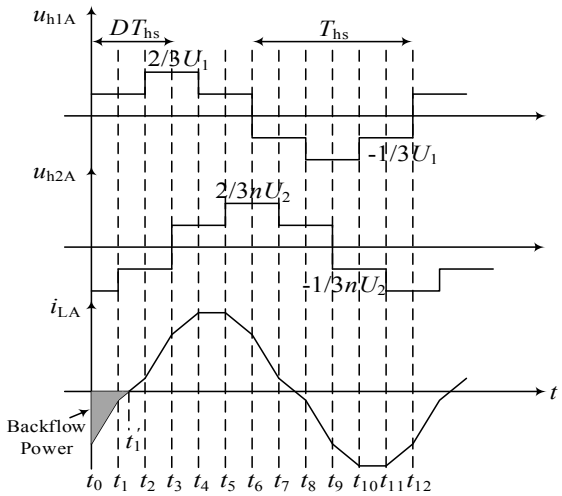

(c) three-phase DAB: π/3<φ<2π/3, 1/3<D<2/3

FIGURE II. OPERATING WAVEFORMS OF CONVERTERS BASED ON THE TRADITIONAL PHASE-SHIFTING CONTROL

TABLE I. THE FIRST KIND OF CIRCUMSTANCE

Operation Modes	Inductive Current
t_0-t_1	$i_L(t_0)+\frac{\frac{U_1}{3}+\frac{nU_2}{3}}{L}(t-t_0)$
t_1-t_2	$i_L(t_1)+\frac{\frac{U_1}{3}-\frac{nU_2}{3}}{L}(t-t_1)$
t_2-t_3	$i_L(t_2)+\frac{\frac{2U_1}{3}-\frac{2nU_2}{3}}{L}(t-t_2)$
t_3-t_4	$i_L(t_3)+\frac{\frac{2U_1}{3}-\frac{2nU_2}{3}}{L}(t-t_3)$
t_4-t_5	$i_L(t_4)+\frac{\frac{U_1}{3}-\frac{2nU_2}{3}}{L}(t-t_4)$
t_5-t_6	$i_L(t_5)+\frac{\frac{U_1}{3}-\frac{nU_2}{3}}{L}(t-t_5)$

TABLE II. THE SECOND KIND OF CIRCUMSTANCE

Operation Modes	Inductive Current
t_0-t_1	$i_L(t_0)+\frac{\frac{U_1}{3}+\frac{2nU_2}{3}}{L}(t-t_0)$
t_1-t_2	$i_L(t_1)+\frac{\frac{U_1}{3}+\frac{nU_2}{3}}{L}(t-t_1)$
t_2-t_3	$i_L(t_2)+\frac{\frac{2U_1}{3}+\frac{nU_2}{3}}{L}(t-t_2)$
t_3-t_4	$i_L(t_3)+\frac{\frac{2U_1}{3}-\frac{nU_2}{3}}{L}(t-t_3)$
t_4-t_5	$i_L(t_4)+\frac{\frac{U_1}{3}-\frac{nU_2}{3}}{L}(t-t_4)$
t_5-t_6	$i_L(t_5)+\frac{\frac{U_1}{3}-\frac{2nU_2}{3}}{L}(t-t_5)$

III. Analysis Of the Power Characteristics of Converters

A. Establishment Of the Mathematical Models

1) Mathematical models of three-phase dual active bridge bi-directional DC-DC converter

According to the operation modes analysis on three-phase DAB by taking A phase as the example in chapter 2. t_0=0 is given; And voltage regulating ratio and switching frequency are set as $k=U_1/(nU_2)\geq 1$ and $f_s=1/(2T_{hs})$, respectively. Therefore, symmetry of $i_L(t_0)=-i_L(t_6)$ is obtained.

(1) When $0<\varphi<\pi/3$, $0<D<1/3$, each moment can be presented as $t_1=DT_{hs}$, $t_2=1/3T_{hs}$, $t_3=(1/3+D)T_{hs}$, $t_4=2/3T_{hs}$, $t_5=(2/3+D)T_{hs}$, $t_6=T_{hs}$. According to the Table I, it can be obtained:

$$i_L(t_0)=-\frac{nU_2}{2f_sL}(\frac{D}{3}+\frac{2}{9}k-\frac{2}{9}) \tag{1}$$

$$i_L(t_1)=\frac{nU_2}{2f_sL}(\frac{D}{3}k-\frac{2}{9}k+\frac{2}{9}) \tag{2}$$

$$i_L(t_2)=\frac{nU_2}{2f_sL}(\frac{D}{3}-\frac{1}{9}k+\frac{1}{9}) \tag{3}$$

$$i_L(t_3)=\frac{nU_2}{2f_sL}(\frac{2D}{3}k-\frac{1}{9}k+\frac{1}{9}) \tag{4}$$

$$i_L(t_4)=\frac{nU_2}{2f_sL}(\frac{2D}{3}+\frac{1}{9}k-\frac{1}{9}) \tag{5}$$

$$i_L(t_5)=\frac{nU_2}{2f_sL}(\frac{D}{3}\mathrm{k}+\frac{1}{9}k-\frac{1}{9}) \tag{6}$$

$$i_L(t_6)=\frac{nU_2}{2f_sL}(\frac{D}{3}+\frac{2}{9}k-\frac{2}{9}) \tag{7}$$

Regarding A-phase power, then:

$$P_A=\frac{1}{T_{hs}}[\frac{U_1}{3}\int_{t_0}^{t_2}i_L(t)\mathrm{d}t+\frac{2U_1}{3}\int_{t_2}^{t_4}i_L(t)\mathrm{d}t+\frac{U_1}{3}\int_{t_4}^{t_6}i_L(t)\mathrm{d}t] \tag{8}$$

Equation (1) - (7) are substituted into the above formula respectively, A-phase transmitted power can be obtained:

$$P_A=\frac{nU_1U_2}{6f_sL}(-\frac{1}{2}D^2+\frac{2}{3}D) \tag{9}$$

Of which, if D=1/3, then:

$$P_{Amax}=\frac{nU_1U_2}{36f_sL} \tag{10}$$

Similarly, regarding three-phase symmetric circuit, then:

$$P_A=P_B=P_C=\frac{nU_1U_2}{6f_sL}(-\frac{1}{2}D^2+\frac{2}{3}D) \tag{11}$$

Then, total transmitted power is:

$$P=\frac{nU_1U_2}{2f_sL}(-\frac{1}{2}D^2+\frac{2}{3}D) \tag{12}$$

According to the backflow defined in chapter 2, A-phase backflow power can be obtained:

$$\begin{aligned}P_{cirA}&=\frac{1}{T_{hs}}\int_0^{t_0'}u_{h1A}\left|i_L(t)\right|\mathrm{d}t\\&=\frac{nU_1U_2}{4f_sL(1+k)}(\frac{1}{3}D+\frac{2}{9}k-\frac{2}{9})^2\end{aligned} \tag{13}$$

In fact, if the inductive current has been reduced to 0 prior to t_0, then backflow power P_{cirA}=0. For the moment, $i_L(t_0)\geq 0$ is given, namely:

$$k\leq 1-\frac{3}{2}D \tag{14}$$

Considering the correlation between the backflow power and the transmitted power, A-phase backflow power ratio M_{cirA} can be defined as:

$$M_{cirA}=\frac{P_{cirA}}{P_A}=\frac{3(1/3D+2/9k-2/9)^2}{(1+k)(-D^2+\frac{4}{3}D)} \tag{15}$$

According to formula (14), constraint conditions of formula (13) can be obtained:

$$k>1-\frac{3}{2}D \tag{16}$$

Similarly:

$$M_{\text{cir}} = M_{\text{cirA}} = M_{\text{cirB}} = M_{\text{cirC}} \tag{17}$$

(2) When $\pi/3<\varphi<2\pi/3$ and $1/3<D<2/3$, each moment can be presented as $t_1=(D-1/3)T_{\text{hs}}$, $t_2=1/3T_{\text{hs}}$, $t_3=DT_{\text{hs}}$, $t_4=2/3T_{\text{hs}}$, $t_5=(1/3+D)T_{\text{hs}}$, $t_6=T_{\text{hs}}$. According to Table II, it can be obtained:

$$i_L(t_0) = -\frac{nU_2}{2f_sL}(\frac{2D}{3}+\frac{2}{9}k-\frac{1}{3}) \tag{18}$$

$$i_L(t_1) = \frac{nU_2}{2f_sL}(\frac{D}{3}k-\frac{1}{3}k+\frac{1}{9}) \tag{19}$$

$$i_L(t_2) = \frac{nU_2}{2f_sL}(-\frac{D}{3}-\frac{1}{9}k+\frac{1}{3}) \tag{20}$$

$$i_L(t_3) = \frac{nU_2}{2f_sL}(\frac{2D}{3}k-\frac{1}{3}k+\frac{2}{9}) \tag{21}$$

$$i_L(t_4) = \frac{nU_2}{2f_sL}(\frac{D}{3}+\frac{1}{9}k) \tag{22}$$

$$i_L(t_5) = \frac{nU_2}{2f_sL}(\frac{D}{3}k+\frac{1}{9}) \tag{23}$$

$$i_L(t_6) = \frac{nU_2}{2f_sL}(\frac{2D}{3}+\frac{2}{9}k-\frac{1}{3}) \tag{24}$$

Regarding A-phase power, there are:

$$P_{\text{A}} = \frac{1}{T_{\text{hs}}}[\frac{U_1}{3}\int_{t_0}^{t_2} i_L(t)\,\mathrm{d}t + \frac{2U_1}{3}\int_{t_2}^{t_4} i_L(t)\,\mathrm{d}t + \frac{U_1}{3}\int_{t_4}^{t_6} i_L(t)\,\mathrm{d}t] \tag{25}$$

Equation (17) - (23) are substituted into the above formula respectively, A-phase transmitted power can be obtained:

$$P_{\text{A}} = \frac{nU_1U_2}{6f_sL}(-D^2+D-\frac{1}{18}) \tag{26}$$

Of which D = 1/2, then:

$$P_{\text{Amax}} = \frac{7nU_1U_2}{216f_sL} \tag{27}$$

Similarly:

$$P_{\text{A}} = P_{\text{B}} = P_{\text{C}} = \frac{nU_1U_2}{6f_sL}(-D^2+D-\frac{1}{18}) \tag{28}$$

Total transmitted power of three-phase is:

$$P = \frac{nU_1U_2}{2f_sL}(-D^2+D-\frac{1}{18}) \tag{29}$$

A-phase backflow power can be obtained according to backflow power defined in article 1.1:

$$\begin{aligned} P_{\text{cirA}} &= \frac{1}{T_{\text{hs}}}\int_0^{t_0'} u_{\text{h1A}}\left|i_L(t)\right|\mathrm{d}t \\ &= \frac{nU_1U_2(\frac{1}{3}D^2-\frac{1}{6}D^2k+\frac{1}{3}Dk-\frac{1}{3}D-\frac{5}{54}k+\frac{2}{27})^2}{6f_sL} \\ &+ \frac{nU_1U_2}{4f_sL(1+k)}(\frac{1}{3}Dk-\frac{1}{3}k+\frac{1}{9})^2 \end{aligned} \tag{30}$$

Considering size correlation between backflow power and transmitted power, M_{cirA} backflow ratio of A-phase defined is:

$$\begin{aligned} M_{\text{cirA}} &= \frac{P_{\text{cirA}}}{P_{\text{A}}} = \frac{\frac{1}{3}D^2-\frac{1}{6}D^2k+\frac{1}{3}Dk-\frac{1}{3}D-\frac{5}{54}k+\frac{2}{27}}{-D^2+D-\frac{1}{18}} \\ &+ \frac{3}{2(1+k)(-D^2+D-\frac{1}{18})}(\frac{1}{3}Dk-\frac{1}{3}k+\frac{1}{9})^2 \end{aligned} \tag{31}$$

Similarly:

$$M_{\text{cir}} = M_{\text{cirA}} = M_{\text{cirB}} = M_{\text{cirC}} \tag{32}$$

2) Mathematical models of single-phase dual active bridge Bi-directional DC-DC converter

It can be obtained from Figure II(a) that there are four working states for single-phase DAB. Analysis process of which is similar to that of three-phase DAB. Transmitted power of single-phase DAB under the traditional phase-shifting control analysis can be obtained:

$$P = \frac{nU_1U_2}{2f_sL}D(1-D) \tag{33}$$

Backflow power is:

$$P_{\text{cir}} = \frac{nU_1U_2[k+(2D-1)]^2}{16f_sL(k+1)} \tag{34}$$

Ratio of backflow power is:

$$M_{\text{cir}} = \frac{P_{\text{cir}}}{P} \frac{[k+(2D-1)]^2}{8(k+1)D(1-D)} \tag{35}$$

B. *Comparative Analysis of Transmitted Power and Backflow Power*

Regarding three-phase DAB, A-phase is also taken as an example to carry out comparative analysis on regulation range of transmitted power that is normalized for convenient analysis. Comparing size of (10) with that of (27), it can be determined that the maximum transmitted power is the standard power P_{N}, then:

$$P_{\text{N}} = \frac{7nU_1U_2}{216 f_{\text{s}} L} \tag{36}$$

According to the (9), (26) and (36), the curve relationship of three-phase DAB standard transmitted power P' changing along with phase-shifting ratio D is shown in Figure III(a).

Similarly, standard power of single-phase DAB is:

$$P_{\text{N}} = \frac{nU_1U_2}{2 f_{\text{s}} L} \tag{37}$$

According to (33) and (37), the curve relationship of single-phase DAB standard transmitted power P' changing along with shift phase ratio D is shown in Figure III(b).

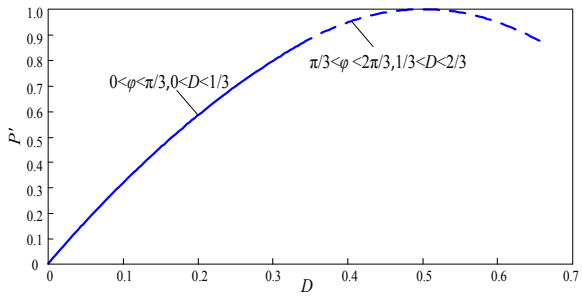

(a) three-phase DAB

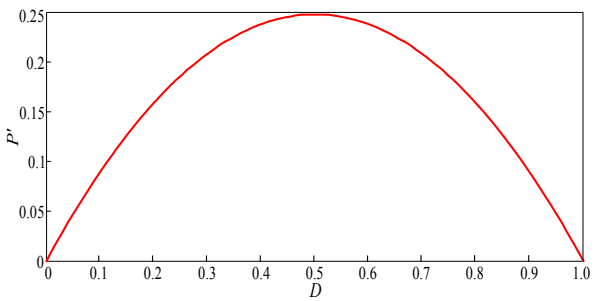

(b) single-phase DAB

FIGURE III. ADJUSTMENT CURVES OF TRANSMITTED POWER

Regulating curve of three-phase DAB transmitted power, by Figure III(a), is divided into two sections. And transmitted power increases along with increase of D before D=0.5; It reaches the maximum when D=0.5; It decreases along with increase of D when D>0.5. Regulating curve of three-phase DAB transmitted power, by Figure III(b) is parabolic. Transmitted power also reaches the maximum when D =0.5.

Assuming that transmitted power of single-phase DAB and that of three-phase DAB are 6KW, respectively. Phase-shifting ratio of closed-loop controlled single-phase DAB is 0.19, while that of three-phase DAB is 0.3. Variation curve of backflow power ratio M_{cir} along with voltage regulation ratio k, as shown in Figure IV.

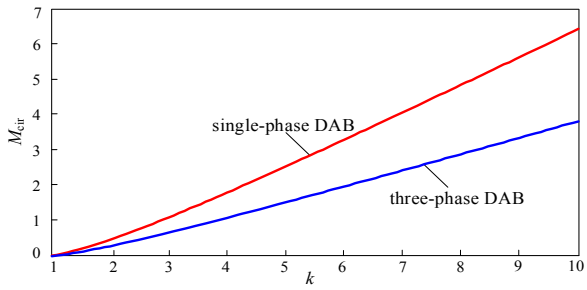

FIGURE IV. CURVE OF BACKFLOW POWER RATIO VARIED WITH VOLTAGE REGULATION RATIO

Backflow power ratio of both, by Figure IV, are increasing along with increase of voltage regulating ratio k under the traditional phase–shifting control; At the same k value, backflow power ratio of three-phase DAB is smaller under same transmitted power, which indicates that power transmitted efficiency of three-phase DAB is higher; At the same time, differences of backflow power ratio between single-phase DAB and three-phase DAB increases gradually along with increase of k.

IV. SIMULATION

Single and three-phase DAB simulation models are built in EMTDC/PSCAD respectively, so as to verify working waveforms, transmission power and backflow power ratio relationship of single-phase DAB and three-phase DAB.

A. *Simulation Parameters*

Simulation parameters for single-phase DAB system are shown in Table III. Voltage outer-loop control is adopted in its voltage control strategy of the output side; control block diagram is shown in Figure V. Simulation parameters for three-phase DAB system are shown in Table IV. Its voltage control strategy of the output side is consistent with that of single-phase DAB.

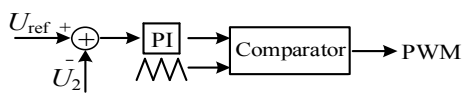

FIGURE V. CONTROL BLOCK DIAGRAM

TABLE III. SYSTEM PARAMETERS OF SINGLE-PHASE DAB

	Value
Input Voltage (V)	1000
Output Voltage (V)	500
Transmission Power (W)	6
Switching Frequency (kHz)	10
Inductance (mH)	1.57
Capacitor (μF)	1100
Transformation Ratio	2

TABLE IV. SYSTEM PARAMETERS OF THREE-PHASE DAB

	Value
Input Voltage (V)	1000
Output Voltage (V)	500
Transmission Power (W)	6
Switching Frequency (kHz)	10
Inductance (mH)	2.6
Capacitor (μF)	1100
Transformation Ratio	2

B. Simulation Results

1) Operating waveforms

Voltage waveforms and the inductive current waveform of single-phase DAB and three-phase DAB in the primary and secondary side can be obtained via simulation, as shown in Figure VI. Voltage waveforms and current waveform on both ends of inductance of single-phase DAB are presented in Figure VI (a-b), of which, voltage waveforms in primary and secondary side belong to square waveforms in high-frequency; Voltage waveforms and current waveforms on both ends of inductance of three-phase DAB presented in Figure VI (c-d), of which, voltage waveform in primary and secondary side belong to high-frequency multi-level waveforms. The simulation results are consistent with the working waveform of traditional shift phase control on single-phase DAB and three-phase DAB as shown in Figure II.

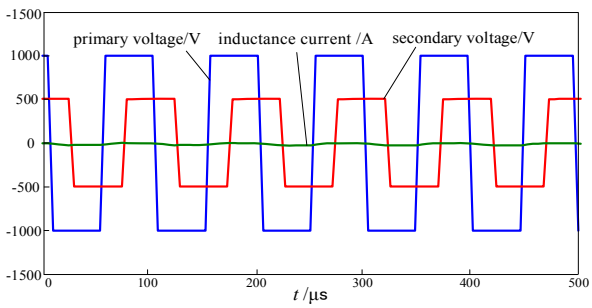

(a) Waveforms of voltage and inductive current of single-phase DAB

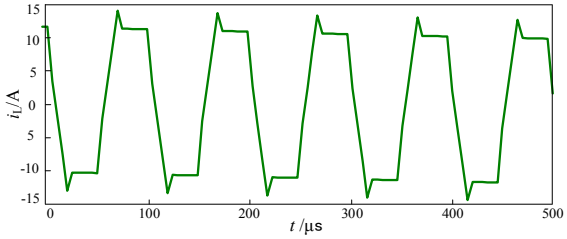

(b) Waveform of inductive current of single-phase DAB

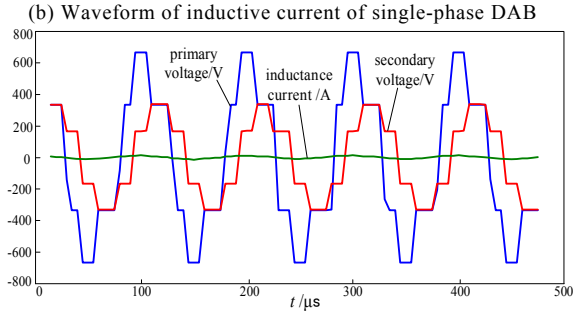

(c) Waveforms of voltage and inductive current of three-phase DAB

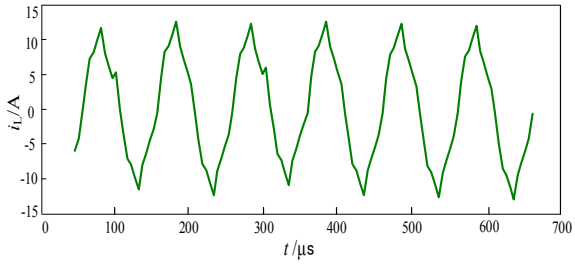

(d) Waveform of inductive current of three-phase DAB

FIGURE VI. SIMULATED SWITCHING WAVEFORMS FOR SINGLE AND THREE-PHASE DAB: 1000VDC INPUT, 400VDC OUTPUT

2) The adjustment curves of transmitted power

Regulating curve verification Figure of single-phase DAB and three-phase DAB transmitted power can be obtained in verifying simulation of regulating curve for transmitted power, as shown in Figure VII. In Figure VII, transmitted powers of single-phase DAB and three-phase DAB reach their maximum when shift phase ratio D = 0.5 that is consistent with (9), (26) and (33) obtained through theoretical analysis as well as regulating curve of transmitted power shown in Figure III.

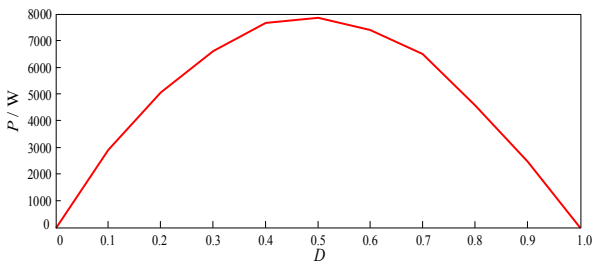

(a) single-phase DAB

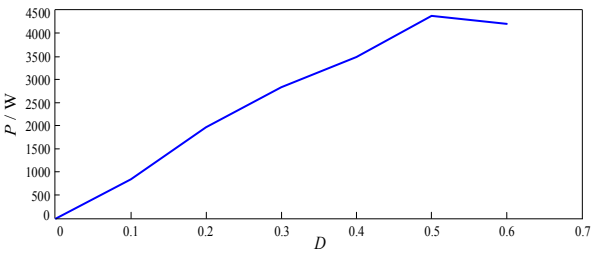

(b) three-phase DAB

FIGURE VII. THE VALIDATION OF THE ADJUSTMENT CURVES OF TRANSMITTED POWER

3) *Backflow power ratio*

Instantaneous power waveform of single-phase DAB and three-phase DAB can be obtained in the simulation of verifying backflow power ratio, as shown in Figure VIII. The part below 0 in the Figure is the backflow power. Smaller backflow power of three-phase DAB and higher power transmitted efficiency can be obtained by Figure VIII, which is consistent with the conclusion gained in Figure IV.

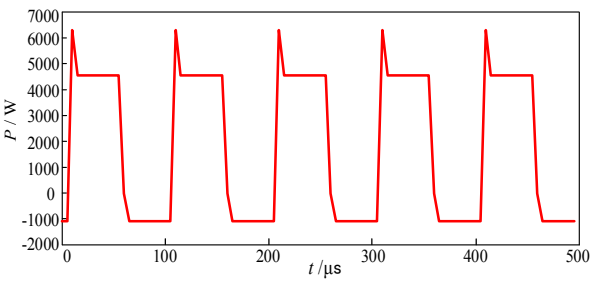

(a) single-phase DAB

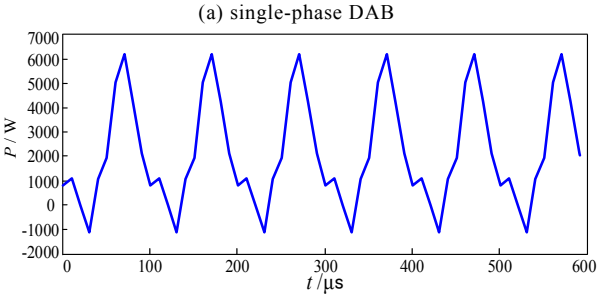

(b) three-phase DAB

FIGURE VIII. WAVEFORMS OF INSTANTANEOUS POWER OF CONVERTERS

V. CONCLUSION

The paper introduces the operating principles of single-phase DAB and three-phase DAB under traditional phase-shifting control and builds mathematical models for transmitted power and backflow power through giving out analysis on working states of a converter. By comparison of DAB backflow power of single-phase DAB and three-phase power, three-phase DAB is with a smaller backflow power and its transmitted efficiency is higher than that of single-phase DAB when transmitted power remains constant. Simulation models of single-phase DAB and three-phase DAB are finally built in EMTDC/PSCAD respectively to verify the working waveforms, regulating curve of transmitted power and backflow power ratio relationship of single-phase DAB and three-phase DAB.

ACKNOWLEDGMENT

This work was supported by the National Natural Science Foundation of China (51277024).

REFERENCES

[1] Qiang SONG, Biao ZHAO, Wenhua LIU, Yuming ZHAO, "Next-generation high-frequency-isolation power conversion technology for smart grid," Proceedings of the CSEE, vol. 34, pp. 6369-6379, 2014.

[2] J. M. Guerrero, J. C. Vasquez, J. Matas, et al. "Control strategy for flexible microgrid based on parallel line-interactive UPS system," IEEE Transactions on Industrial Electronics, vol. 56, pp. 726-736, 2009.

[3] H. C. Chiang, T. T. Ma, Y. H. Cheng, J. M. Chang, W. N. Chang, "Design and implementation of a hybrid regenerative power system combining grid-tie and uninterruptible power supply functions," IET Renewable Power Generation, vol. 4, pp. 85-99, 2009.

[4] Mingrui ZHANG, Jinhui LIU, Xin JIN, "Research on the FREEDM micro-grid and its relay protection," Power System Protection and Control, vol. 39, pp. 95-99, 2011.

[5] Li LI, Gang LIU, "Development of bi-directional DC-DC converter in multiple battery energy storage system," Power System Protection and Control, vol. 39, pp. 90-94, 2011.

[6] Chunshui DU, Chenghui ZHANG, Alian CHEN, Fangde ZHAO, Weirong XIAO, "Digital control and implementation of photovoltaic soft-switching DC-DC converter with high-frequency step-up transformer isolation," Transactions of China Electrotechnical Society, vol. 26, pp. 57-63, 2011.

[7] Mingrui ZHANG, Chengxin LIN, Ruixin XU, "Grid-connected photovoltaic power generation technology based on SST," Power System Protection and Control, vol. 40, pp. 133-138, 2012.

[8] Biao ZHAO, Qingguang YU, Weixin SUN, "Bi-directional full-bridge DC-DC converters with dual-phase-shifting control and its backflow power characteristic analysis," Proceedings of the CSEE, vol. 32, pp. 43-50, 2012.

[9] Xun ZHANG, Guangzhu WANG, Xiujuan SHANG, Ting WANG, "An optimized strategy based on backflow power of bi-directional dual-active-bridge DC-DC converters with dual-phase-shifting control," Proceedings of the CSEE, vol. 36, pp. 1090-1097, 2016.

[10] Lin WU, Zhigang LIU, Xiang HONG, "Comparison and analysis of power control characteristic for isolated bidirectional full-bridge DC-DC converter," Transactions of China Electrotechnical Society, vol. 28, pp. 179-187, 2013.

[11] Chunfang WANG, Qinchao XU, "Study of LLC resonant converter for variable-frequence microwave oven power supply," Transactions of China Electrotechnical Society, vol. 27, pp. 103-109, 2012.

[12] Hong ZHU, Huilong ZHOU, Liangliang REN, Ling GU, Ke JIN, "A three-phase bidirectional DC-DC converter based on phase shift control," Transactions of China Electrotechnical Society, vol. 30, pp. 39-46, 2015.

[13] H. B. Nico, E. Everts, G. E. W. Cornelis, A. L. Elena, "Performance evaluation of a three-phase dual active bridge DC–DC converter with different transformer winding configurations," IEEE Transactions on Power Electronics, vol. 31, pp. 6814-6823, 2016.

[14] H. R. E. Larico, I. Barbi, "Three-phase push-pull DC-DC converter: analysis, design, and experimentation," IEEE Transactions on Industrial Electronics, vol. 59, pp. 4629-4636, 2012.

[15] R. L. Andersen, I. Barbi, "A ZVS-PWM three-phase current-fed push/pull DC/DC converter," IEEE Transactions on Industrial Electronics, vol. 60, pp. 838-847, 2013.